JAERI-M

5502

CONCEPTUAL DESIGN OF A GAS COOLED TOKAMAK REACTOR

December 1973

Kiyoshi SAKO, Mitsuru OHTA, Yasushi SEKI
Harumi YAMATO*, Toru HIRAOKA, Kichizo TANAKA,
Naoto ASAMI** and Sigeru MORI

日本原子力研究所
Japan Atomic Energy Research Institute

この報告書は，日本原子力研究所がJAERI-Mレポートとして，不定期に刊行している研究報告書です．入手，複製などのお問合わせは，日本原子力研究所技術情報部（茨城県那珂郡東海村）あて，お申しこしください．

JAERI-M reports, issued irregularly, describe the results of research works carried out in JAERI. Inquiries about the availability of reports and their reproduction should be addressed to Division of Technical Information, Japan Atomic Energy Research Institute, Tokai-mura, Naka-gun, Ibaraki-ken, Japan.

ガス冷却型トカマク炉の試設計

日本原子力研究所東海研究所核融合研究室

迫　　淳・太田　充・関　　泰

大和　春海*・平岡　徹(1)・田中吉左右(2)

浅見　直人**・森　　茂

（１９７３年１２月８日受理）

ヘリウム冷却型トカマク炉の試設計を行ない，炉心プラズマ，炉構造，ブランケット物理，材料について評価した。この炉の主要設計パラメータは次のとおりである；炉出力２０００MWt，第１壁熱負荷2MW／m^2，プラズマ主／副半径１０／２m，平均トロイダル磁束密度６０kG，炉入口／出口冷却体温度４００／６００℃，ブランケット親物質Li_2Oペブル，第１壁材料インコロイ８００。

---

(1) 原子炉工学部高速炉物理研究室

(2) 製造部製造技術課

* 外来研究員（東芝，総合研究所）

** 協力研究員（三菱原子力，研究所）

（本報告書は１９７４年１月２９日～２月１５日英国カラム研究所で開かれるＩＡＥＡ主催の“核融合炉設計上の問題”に関するワークショップに討議用として提出するために用意したものである。

目　次　な　し

CONCEPTUAL DESIGN OF A GAS COOLED TOKAMAK REACTOR

Kiyoshi SAKO, Mitsuru OHTA, Yasushi SEKI
Harumi YAMATO*, Toru HIRAOKA, Kichizo TANAKA,
Naoto ASAMI** and Sigeru MORI

Tokai Research Establishment, JAERI
Tokai-mura, Naka-gun, Ibaraki, Japan

(Received December 8, 1973)

Abstract

A conceptual design of a helium cooled tokamak reactor has been carried out. Core plasma, reactor structure, blanket neutronics and material of the reactor are evaluated.

The main design parameters of the fusion reactor are as follows; reactor output 2000 MWt, first wall loading 2 MW/m^2, plasma major/minor radius 10/2m, average toroidal magnetic field 60 kG and reactor inlet/outlet coolant temperature 400/600°C. Li_2O pebble and Incoloy 800 are used for the blanket fertile material and the first wall material, respectively.

1. General

A conceptual design of a gas cooled tokamak reactor has been carried out in order to clarify the problems on the fusion power reactor development.

The main design parameters are shown in Table 1.1 and the overall view of the reactor is shown in Fig.1.1. The detailed arrangement of the blanket is shown in Fig.1.2, schematically.

The reactor output (2000 MW) and the plasma dimensions (R=10m, a=2m) were selected by compromizing the plasma characteristics, the reactor structural consideration, the allowable maximum toroidal magnetic field and the first wall loading, etc.

---

* On leave from Research and Development Center, Tokyo Shibaura Electric Co. Ltd., Kawasaki.

** On leave from Engineering and Development Division, Mitsubishi Atomic Power Industries Inc., Ohmiya.

This paper was prepared for submittal to IAEA Workshop on " Fusion Reactor Design Problems ", UKAEA Culham laboratory, Abingdon, Berkshire, England, 29 Jan. to 15 Feb. 1974.

In this paper we discuss the following problems;

1) Core plasma; The plasma parameters were decided by assuming the circular cross sectional plasma and the plasma characteristics were analyzed for the steady state and transient state conditions. The necessity of a divertor and its concept were also studied preliminarily.
2) Reactor structural design; A helium cooled reactor system which has the blanket of Li_2O pebbles and graphite balls was selected. This concept was selected to simplify the blanket structure. The thermal and mechanical evaluations were carried out.
3) Blanket nuclear design; The heat generation and the tritium breeding in the blanket for the prescribed concept were evaluated.
4) Material considerations; The first wall material of Incoloy 800 and the blanket fertile material of Li_2O were evaluated. Tritium recovery from the blanket was also studied.

Table 1.1 Main Design Parameters

Power	:	Reactor Thermal Output	2000 MW
		Electrical Output	800 MW
		First Wall Loading	2 MW m^{-2}
Reactor Dimensions	:	Torus Major Radius	10 m
		Plasma Radius	2 m
		First Wall Radius	2.5 m
Plasma Parameters	:	Plasma Temperature	15 keV
		Plasma Density	1.1×10^{14} cm^{-3}
		Plasma Current	8 MA
		Confinement Time	2.3 sec
		Toroidal Magnetic Field (Average)	60 kG
		Operation Period	100 min
Blanket Material	:	Structural Material (1st Wall)	Incoloy 800
		Fertile Material	Li_2O Pebble
		Reflector Material	Graphite Ball
Neutronics	:	First Wall Neutron Flux (Total)	2.7×10^{14}n $cm^{-2}s^{-1}$
		Tritium Breeding Ratio	1.16
Cooling System	:	Coolant, Pressure	He, 20 ata
		Reactor Inlet/Outlet Temperature	400/600°C

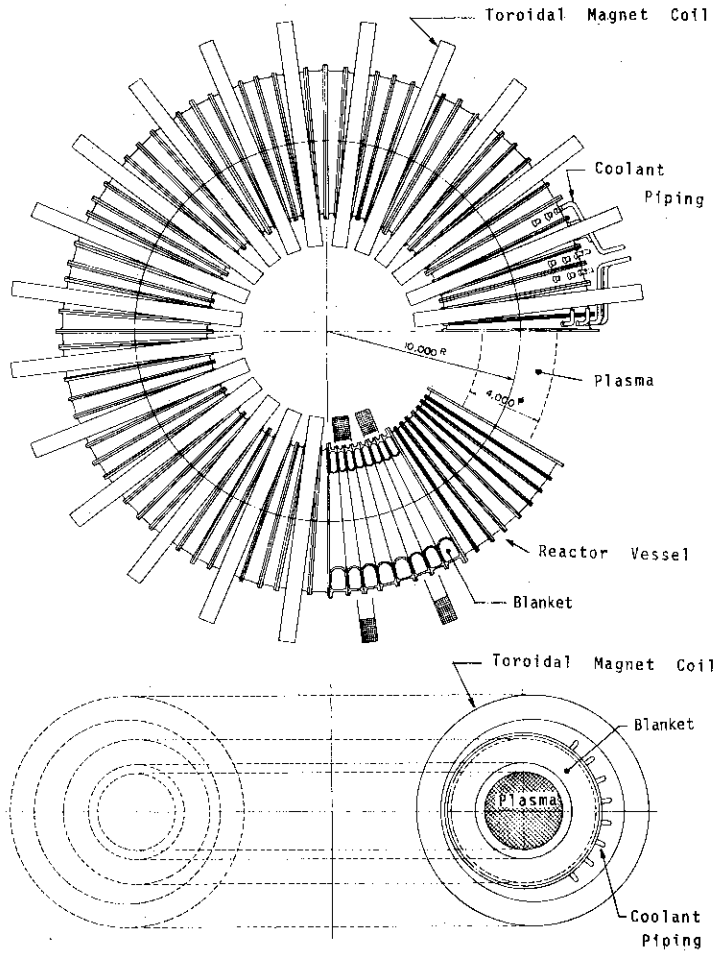

Fig. 1.1 Overall view of the reactor.

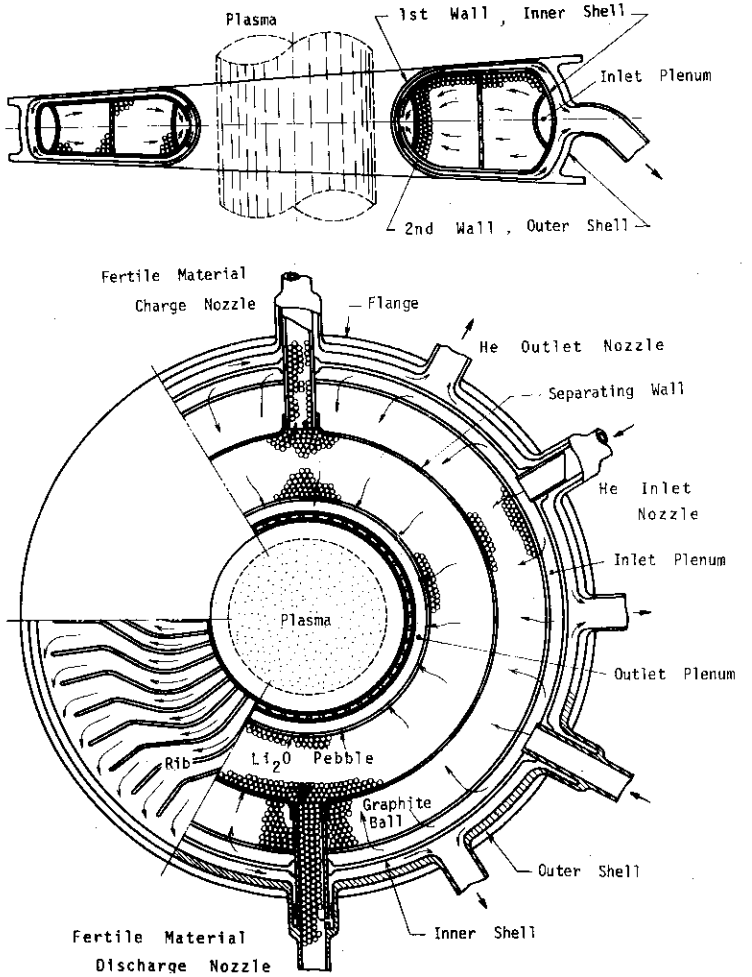

Fig. 1.2 Detailed arrangement of the blanket.

2. Core Plasma

2.1 Plasma Parameters

A steady state operation of the core plasma at T=15 keV is assumed, in which various losses are compensated by a particle heating. A rather large value of 5 is chosen for the aspect ratio A=R/a. When poloidal $\beta_p=2$ and the safety factor q=1.5 are assumed, value of β, which is given by $\beta=\beta_p/(qA)^2$, becomes 3.6 %. The toroidal magnetic field of 60 kG on the axis of the plasma is assumed. As a result the plasma density becomes 1.1×10^{14} cm^{-3} and the power density P_D = 2.6 W/cm^3 is obtained in the plasma volume, Thus the major radius of 10 m is necessary in order to obtain the thermal output of 2000 MW.

The required plasma confinement time τ is calculated from a power balance equation. The values of α heating power, bremsstrahlung loss and synchrotron radiation loss are given in Table 2.1.

In the calculation of P_b, $Z_{eff}=2$(effective Z) is used and the synchrotron radiation is estimated from the equation given by Yang et al.[1] This confinement time is compared with those obtained by various scaling laws in Table 2.1.

2.2 Ignition and Shutdown

The plasma current of 8 MA, which corresponds to q=1.5, is excited and sustained during an operation period of 100 min by a current transformer core. The necessary flux change in the core is 195 Vsec to energized the plasma inductance and is 148 Vsec to sustain plasma current for 100 min at the temperature of 15 keV. The core radius of 4.5 m is used and the magnetic field is changed from -30 to +30 kG.

The neutral injection heating of 30 MW is applied at the temperature of 1 keV and is turned off at 10 keV. The time behavior of the plasma temperature is calculated when the particle confinement time is given by

$$\tau = 6.25 \times 10^{12} \frac{a^2 B_t^{\,2} T_e^{\,1/2}}{A^2 q^2 Z_{eff}\, n} , \qquad T \leq 8 \text{ keV} \qquad (2.1)$$

$$\tau = 9.20 \times 10^{-18} C R^{5/2} a^{3/2} B_t^{\,2} \frac{Z_{eff}\, n}{T_e^{\,7/2}} , \quad T \geq 8 \text{ keV} \qquad (2.2)$$

where a and R are in m, B_t in kG, T_e in keV and n in cm^{-3}. (2.1) corresponds to the pseudoclassical diffusion and (2.2) to the anomalous diffusion given by trapped ion instability. The correction factor C = 1.17 is used so as to obtain the steady state at T = 15 keV. A result is shown in Fig.2.1.

The temperature and density changes are also calculated with time for shutdown phase of the reactor which is shown in Fig.2.2. Confinement of the plasma should not be stopped before the temperature becomes low enough not to damage the first wall. In Fig.2.2 the injection of tritium is stopped at t=0 and injection rate of deuterium is doubled compared with that of steady state.

2.3 Fuel Injection and Extraction

The fuel burn up ratio f_b is about 3 % at a steady state of T=15 keV and the injeciton rate of fuel $S=3.8 \times 10^{22}$ atoms/sec is necessary to keep a steady state density when the particle confinement time is 2.3 sec. In order to obtain $Z_{eff}=2$, the impurity level of the first wall material must be about 0.18 % if Z=26 for impurity ions is assumed. This impurity level is obtained when a divertor with efficiency $\eta_D=95$ % is used to decrease the wall flux of high energy plasma particles. The impurity level is given by $(1-\eta_D)\alpha_i/[1-(1-\eta_D)\alpha_I]$ where α_i and α_I are the sputter ratios of plasma particles and impurity respectively and $\alpha_i=0.03$ and $\alpha_I=3$ are used. A pumping system with 540 torrℓ/sec is necessary to evacuate the divertor region.

Table 2.1 Plasma Parameters

Safety Factor	q	1.5
Aspect Ratio	A	5
Poloidal β Value	β_p	2.0
β Value	β(%)	3.6
Density	$n(cm^{-3})$	1.1×10^{14}
Temperature	T(keV)	15.0
Required Confinement Time	τ(sec)	2.3
Pseudoclassical[2]	τ_p(sec)	29.6
Trapped Ion Inst.[3]	τ_T(sec)	1.9
NeoBohm[4]	τ_{NB}(sec)	1.9
Empirical Scaling	τ_E(sec)	12.4
Plasma Volume	$V_p(cm^3)$	79.0
α Heating Power	P_H(MW)	318
Bremsstrahlung Loss	P_b(MW)	36.4
Synchrotron Radiation Loss	P_s(MW)	8.3
Plasma Current	I_p(MA)	8.0
Magnetic Flux	$L\ I_p$	195
Injection Heating Power	P_{IH}(MW)	30
Fuel Injection Rate	$S(sec^{-1})$	3.8×10^{22}
Burn-up Ratio	f_b(%)	3.0
Effective Z	Z_{eff}	2.0

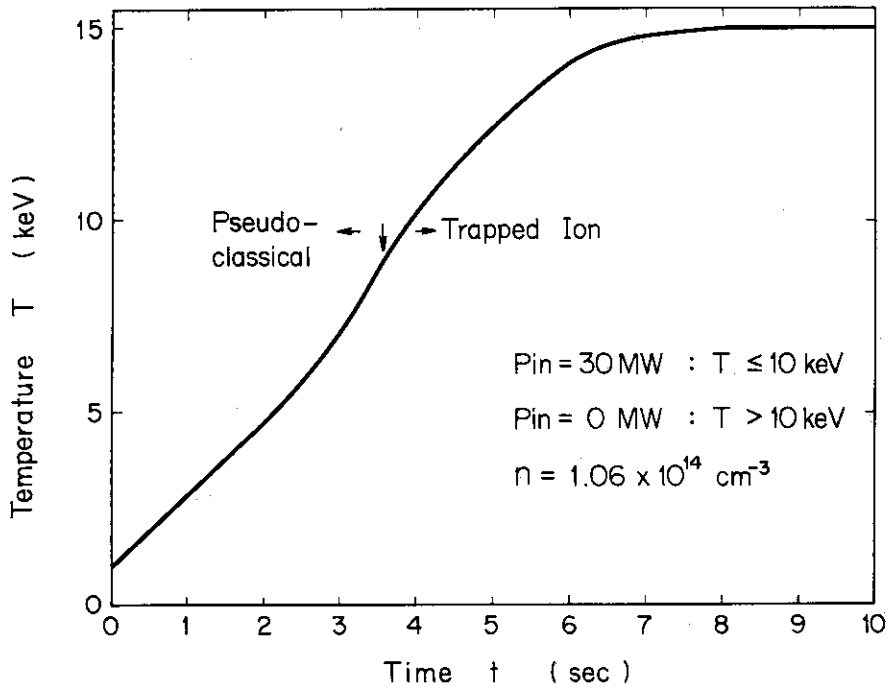

Fig. 2.1 Time dependent behavior of plasma temperature when the heating power of 30MW is injected at T<10 keV and is stopped at T>10 keV. The initial temperature is assumed 1 keV.

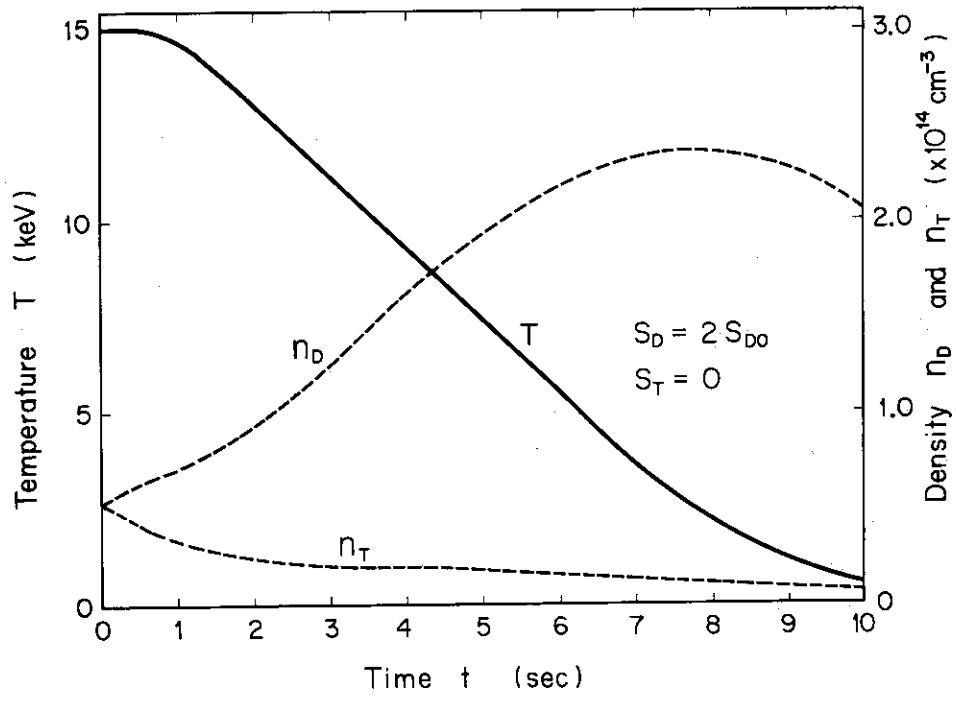

Fig. 2.2 Time dependent behavior of plasma density and temperature at the shutdown of a reactor when the tritium injection is stopped and the deutrium injection rate is doubled.

3. Reactor Structual Design

3.1 Configuration of the Reactor

The overall view of the reactor is shown in Fig.1.1 and the detailed arrangement of the blanket is shown in Fig.1.2. The core plasma diameter is 4 m and the first wall diameter is 5 m. The blanket region is divided into 96 unit cells and each cell is made up of Li_2O pebbles and graphite balls contained in a ring shaped Incoloy vessel. The vessel has a dual shell structure, in which the first wall corresponds to the outer shell and the second to the inner shell. These two walls are connected to each other by ribs and they act as a strengthen member. The space between first wall, second wall and ribs is used for flow channel of He coolant. Flow directions of coolant are shown by arrows in Fig.1.2. The coolant coming into the blanket region flows between graphite balls and Li_2O pebbles and then collected to the outlet nozzle through the flow channels of the first and second walls.

The Li_2O pebbles are used for fertile material and graphite ball for the neutron reflector. As is discussed in §5.3, the recovery of tritium from Li_2O pebbles may only be possible if the pebbles are removed from the blanket and reprocessed. Charge/discharge nozzles for Li_2O pebbles are shown in Fig.1.2. Refueling of Li_2O once or twice a year is necessary, since the tritium production rate is estimated about 100 kg/year. Possibility of tritium recovery from the pebbles placed in the blanket is aslo discussed in the §5.3.

By using the configuration discussed above, the internal structure of the blanket becomes much simpler compared with the system, in which the He cooling pipes are placed in the liquid Li fertile material. On the other hand, a weak point of this configuration is that the large thermal stress is easily induced in the first wall due to restricted thermal expansion. The configuration shown in Fig.3.3 similar to the cell structure proposed by the Culham laboratory[5],[6] may be more favorable if the tritium recovery is possible without replacing the Li_2O pebbles and is now under investigation.

3.2 Temperature and Stress Distributions in the First Wall

The temperature and stress distributions of the first and second walls are calculated for the steady operating condition under simplifying assumptions. The dimemsions of a blanket unit are shown in Fig.3.1.

1) Temperature Distributions

Temperature distributions at the cross section A-A of Fig.3.1 are calculated under the following assumptions.

a) Heat flux on the plasma side of the first wall by plasma particles and various radiations is assumed 6.0 W/cm^2.

b) The values given in Fig.4.3 are used for the heat generation in the wall.
c) The coolant bulk temperature of 550°C is assumed.
d) Three times larger value of heat transfer coefficient than that of fully developed flow is used, as improvement of heat transfer is expected by installing a spoiler in the flow channel, though the experimental verification is necessary.

The temperature distributions are shown in Fig.3.2. According to Fig. 3.2 the average first wall temperature is nearly equal to the coolant outlet temperature of 600°C.

Although the above calculations are performed for nominal values, the hot channel and power peaking factors should be taken into account in more detailed analysis.

2) Pressure and Thermal Stress Distributions

Distributions of stress induced by coolant pressure and temperature difference is calculated at the A-A cross section in the directions "a" and "b" of the Fig.3.1. The direction "a" is along the major circumference of the torus and the direction "b" is along the minor circumference of the torus. The stresses calculated here are only nominal values and the stress concentration is not taken into account.

a) "a" direction

As the radius of curvature of the first wall is much smaller in "a" direction than in "b" direction, the curvature in "b" direction is neglected in the stress calculation. The pressure stress is about 8 kg/mm^2 when the effective thickness of 11 mm, and the radius of curvature of 430 mm are assumed for the wall.

The thermal stress distributions can be calculated from Fig.3.2, since the thermal stress is proportional to difference between the mean and the local temperature. A temperature difference of 10°C corresponds to 4 kg/mm^2 of thermal stress and the mean temperature of the wall is about 600°C in Fig.3.2. The maximum thermal stress obtained is about 12 kg/mm^2.

b) "b" direction

The compressive stress induced by coolant pressure in the "b" direction is small and is neglected. The thermal stress is given by difference between the flange temperature and the local wall temperature, since the expansion of "b" direction is restricted by the flange. In this case the flange temperature and wall mean temperature are the same, so the stress is nearly equal to the thermal stress of "a" direction.

3.3 Transient Consideration

The thermal cycle fatigue must be a severe problem for the first wall

as pulse operation is assumed in our reactor. Change of temperature at A-A section of the first wall after the reactor shut down (step function assumed) is calculated. The wall average temperature drops from 610°C to 570°C in 10sec, while the temperature change of the flange is negligible because of its large heat content and low heat transfer coefficient. As a result the induced average tensile stress in the wall of "b" direction becomes 12 kg/mm^2 because of the temperature difference of 30°C. This result clearly shows that carefull control of the coolant flow rate is indispensable.

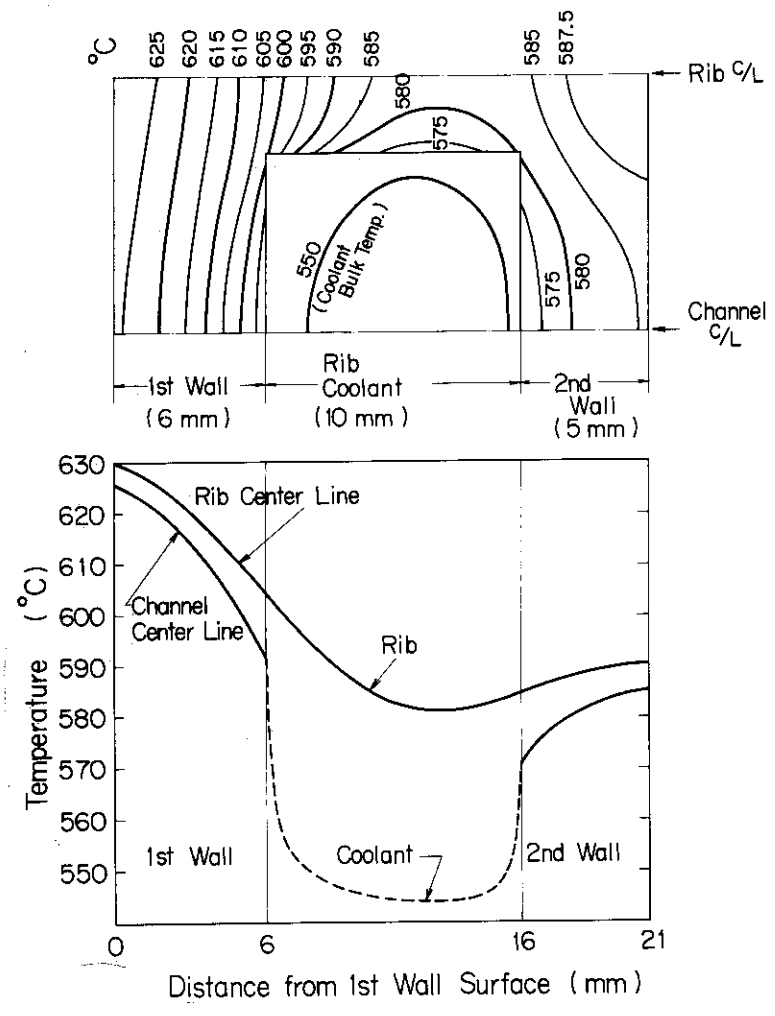

Fig. 3.2 Temperature distributions at the cross section A-A of Fig. 3.1.

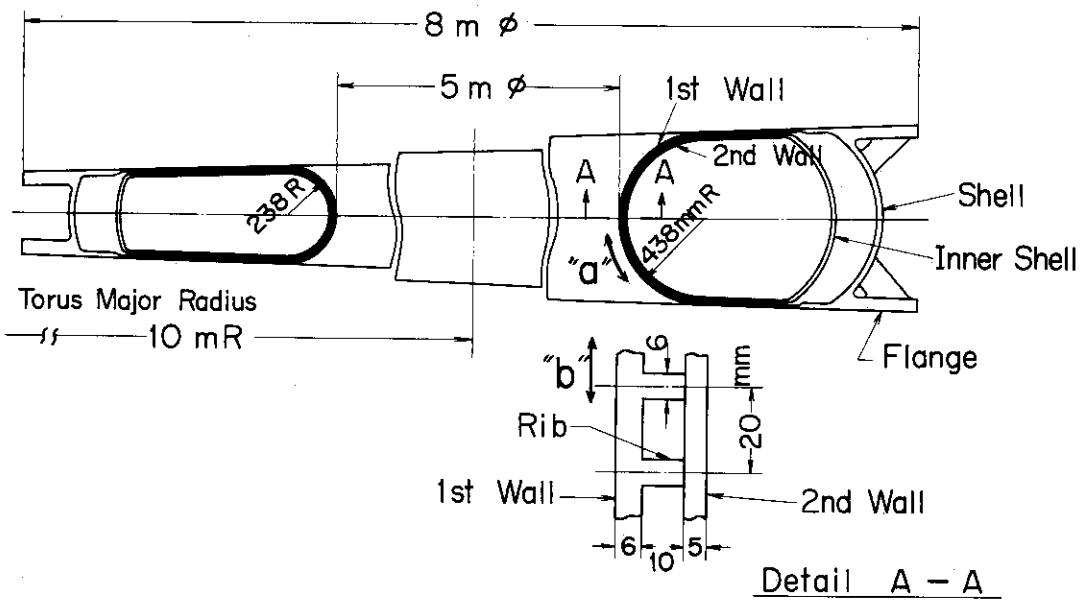

Fig. 3.1 Dimensions of a blanket unit.

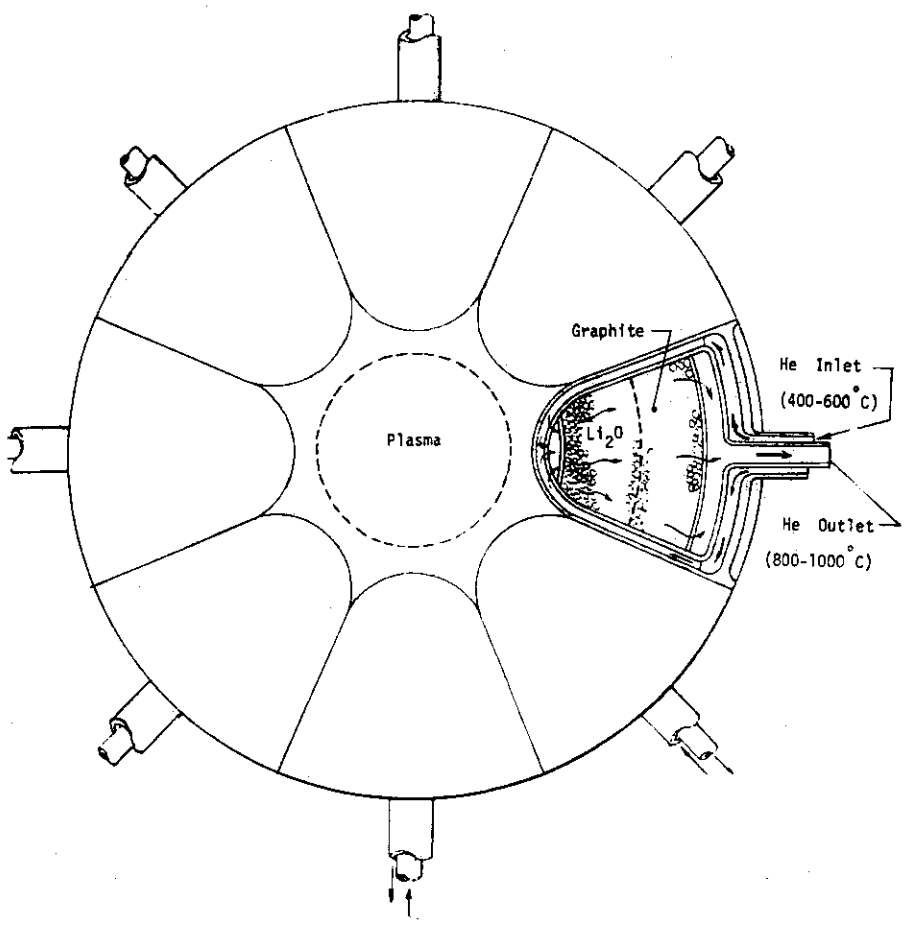

Fig. 3.3 Alternative design concept of the blanket structure.

4. Blanket Nuclear Design

A one-dimensional cylindrical model used in the nuclear calculations of the fusion reactor blanket and the nuclide densities of the homogenized regions, are shown in Fig.4.1. The theoretical density of lithium oxide of 2.01 g/cm^3 is used. It is assumed that plasma and vacuum regions are occupied by helium with the density of 10^{13} atoms/cm^3. Neutron fluxes, gamma-ray fluxes, and reaction rates were calculated by the ANISN[7] code with ENDF/B III data[8]. The S_8 approximation with P_5 anisotropy in 42 neutron energy groups was chosen for neutron fluxes and S_8, P_5 scattering with 21 energy groups was used in treating the gamma fluxes. The details of the compilation of several types of cross sections used in the nuclear heating calculation are described elsewhere[9].

4.1 Tritium Breeding

The distribution of tritium production reaction rates are given in Fig. 4.2. The tritium breeding ratio by ^{6}Li(n,α)t reaction is 0.80 and the tritium breeding ratio by ^{7}Li(n,n'α)t reaction is 0.36. The total tritium breeding ratio of 1.16 is obtained even with relatively thin breeding region of 43 cm.

4.2 Nuclear Heating

Spatially dependent heating rates in the blanket are presented in Fig.4.3. Total nuclear heating rate is represented by solid curve and gamma-ray heating rate is represented by dashed curve. The total heating rate at the first wall is about 22 watts/cm^3. About 60 % of the heat deposit in the first wall arises from gamma rays.

4.3 Magnet Shield Considerations

Although the design study of the shielding for the super-conducting magnet is not yet completed, it seems clear that a sufficiently thick layer for the shielding is available for reducing the neutron flux level below 10^9 n/cm^2 sec in the magnet. Since the breeding region and the reflector occupy only 65 cm in the 150 cm thick blanket, the space of 85 cm remains for the shielding. This space will be thick enough, according to some studies[10],[11] if the accumulated layers of iron and moderator containing boron atoms were employed.

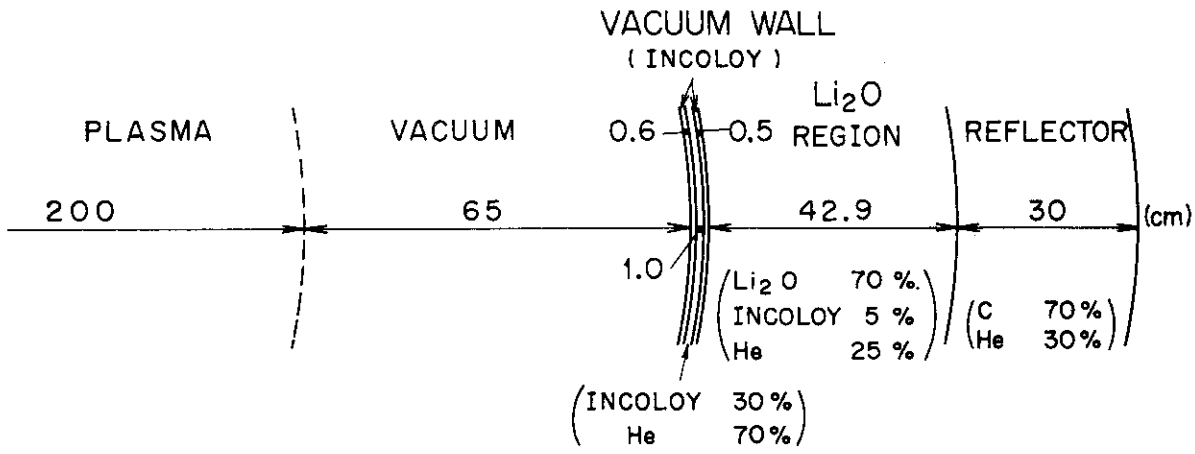

Summary of nuclide densities

Composition	Nuclide Density (atoms/cm^3 x 10^{24})							
	He	Cr	Fe	Ni	^{6}Li	^{7}Li	O	C
1. Plasma	10^{-11}							
2. Vacuum	10^{-11}							
3. INCOLOY		0.01951	0.04021	0.02674				
4. He (70%)	0.00021							
INCOLOY(30%)		0.00585	0.01206	0.00802				
5. INCOLOY		0.01951	0.04021	0.02674				
6. Li_2O (70%)					0.004235	0.05284	0.02354	
INCOLOY(5%)		0.00098	0.00201	0.00134				
He (25%)	0.00008							
7. GRAPHITE(70%)								0.05862
He (30%)	0.00009							

Fig. 4.1 Configuration of the blanket.

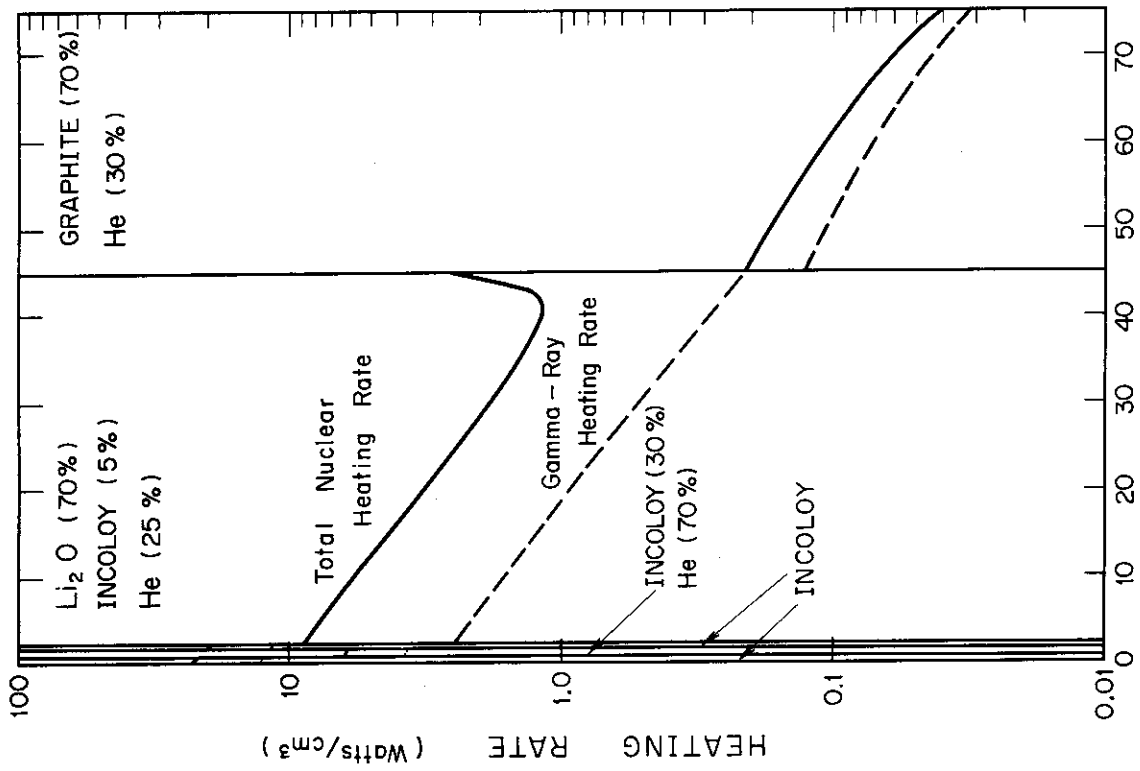

Fig. 4.3 The distribution of nuclear heating rate in the blanket.

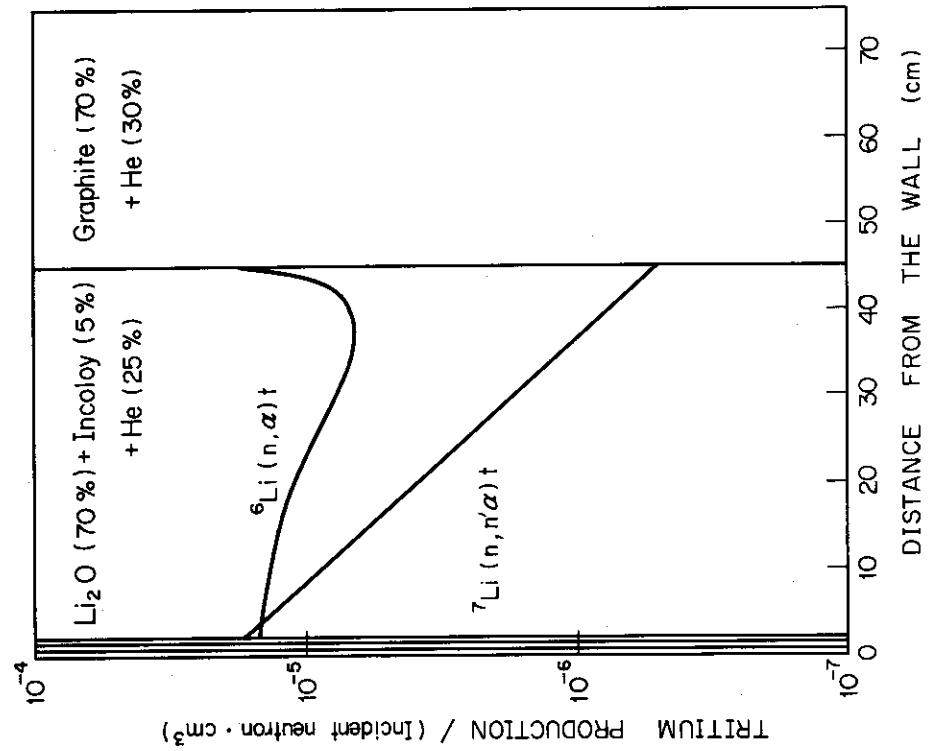

Fig. 4.2 The distribution of tritium production rate in the blanket.

5. Material Considerations

5.1 Reactor Wall Materials

Primary statements for the selection of reactor wall material in this design study are the superiority of high temperature mechanical strength and the availability in present state of material fabrication technology. Incoloy 800 is selected as the suitable material having high corrosion resistance and ductility. 0.2 % yield strength and elongation of hot rolled Incoloy 800 at 593°C are 24.5 kg/m^2 and 40 % respectively, and creep strengh (1 % per 10^5 hours) is 19 kg/mm^2[12].

Neutron flux at the first wall was calculated as $6.3\times10^{13}n/cm^2sec$ for 14 MeV, $1.96\times19^{14}n/cm^2sec$ for E>0.1 MeV and $2.7\times10^{14}n/cm^2sec$ for total neutron. Calculated He and H production rate within the first wall material are 404 ppm/year and 1157 ppm/year respectively, and these values are estimated nearly the same as the case of AISI316 SS. Difference of reaction rates between the plasma side and coolant side of the first wall are about 10 % for both (n,α) and (n,p) reactions. Since radiation damage can cause reduction in strength and ductility, appropriate evaluation of the irradiation behavior of the wall material is of major importance in the design study.

We have, however, little informations concerning the neutron irradiation effects on Incoloy 800. The amount of the swelling of annealed Incoloy 800 irradiated to $2\times10^{22}n/cm^2$(E>0.1 MeV) in EBR-II reacor at 660°C and 757°C are 2.5 % and 0.01 % respectively[13],[14]. It is suggested that Incoloy 800 should be used at higher temperature as far as swelling behavior is concerned. Design study on the fusion reactor with higher operating temperature is now under way as based on prescribed design philosophy.

As another problem arises with pulse operation of tokamak type reactor, thermal cycle fatigue which will be emphasized by neutron irradiation, must be considered. Thermal cycles of 5.25×10^3 times/year are applied to the wall materials due to the pulse operation of 6000 sec/cycle.

Fatigue properties were investigated[15] on irradiated austenitic steal at 700°C in air. Total strain range $\Delta\varepsilon_f$ is reduced to 0.2 % at 10^4 cycle for neutron irradiated Incoloy 800 to $5\times10^{22}n/cm^2$ (E>0.1 MeV). It is suggested from above consideration that further contrivance on the system and structural design will be necessary such that reduction of the thermal stress during periodic operation, prevention of rapid cooling at the reactor shut down, or elongation of pulse period.

First wall erosion according to the sputtering of plasma particles is also estimated. Sputtering ratio for the deuterium and tritium, helium,

neutron and self atoms of austenitic steel are estimated as 0.03[16], 0.15, 0.001[17] and 3[18] atoms/particle respectively. Consideration of the wall area 987 m^2 with uniform radial loss of 5 % of total plasma particles and with averaged burn up ratio of 3.0 % as described before, results in the erosion rate of 0.029 mm/year. Assuming wall integrity is lost after 20 % erosion and the erosion rate for the convex surface is twice lager than the uniform surface, the wall life time will be of the order of 20 years.

5.2 Properties of Lithium Oxide as a Fertile Material

Lithium oxide shows high melting point among the lithium compounds and it is a non-volatile and chemically stable substance. The crystal structure is similar to sodium oxide which is regarded to an ionic crystal. Some physical properties of lithium oxide relevant to the fusion reactor design are listed in Table 5.1. Chemically pure lithium oxide is obtained by the pyrolysis of pure lithium carbonate. The oxide acts as a strong base and reacts violently with CO_2 at several hundred degrees centigrades to form carbonate. Lithium oxide can frequently dissolve various other oxides. For complete design of the oxide fuel fusion blanket, much information on the physical and chemical properties have to be available and particularly we need these mechanical properties and thermal conductivity.

5.3 Tritium Recovery from the Lithium Oxide Blanket

Neutrons generated from the plasma of fusion reactor are absorbed in the blanket to produce tritium. In lithium oxide blanket, tritium may be formed as LiOT. The volatility of LiOT may be low at 600°C, therefore, the tritium inventory increases in an oxide fuel fusion reactor. For reducing tritium inventory fuel pebbles are taken out of the reactor and subjected to reprocessing. Major portion of tritium is effectively separated from the blanket in this process and recovered by following treatment in the plant which is located adjacent to the reactor.

In tritium separation and recovery system on the reprocessing we propose two processes. In one possible process the fuel pebbles are heated at elevated temperature (b.p. of LiOH = 925°C) under evacuation. Vaporized LiOT is trapped by pumping into the column which loads cold trap. Tritium is efficiently recovered as T_2O from the trapped LiOT. The alternative process involves both the conversion of lithium oxide to carbonate by passing preheated carbon dioxide under careful control of gas pressure upon lithium oxide at 200-300°C, and the reconversion of the carbonate to lithium oxide by heating. Tritium liberated from the pebbles as T_2O is effectively recovered from the exhaust gas of these conversion systems.

In order to reduce the reprocessing frequency the tritium recovery on operation of the fusion reactor is considered, that is, a continuous trapping of liberated fraction from the blanket pebbles. However, in this system the operation temperature has to be raised. Another approach is a process without further reprocessing. After shut down of the reactor LiOT is recovered by heating the fuel pebbles under fine control of decay heat removal rate and of reduced helium coolant pressure.

Further possibility to reduce tritium inventory is the application of the continuous recovery of rather liberal components such as T_2 or T_2O formed by the process of the stabilization of energetic T atom in the blanket, however, the fate of T is ambiguous at the present.

Table 5.1 Properties of Lithium Oxide (Fertile Material) and Lithium Hydroxide (Reaction Product)[19],[20],[21]

		Li_2O	LiOT*	
Molecular Weight	(g)	29.88	25.955	
Density	(g cm^{-3} 25°C)	2.013	1.43	
Melting Point	(°C)	1700	445	
Boiling Point	(°C)	2600	925	
Vapor Pressure	(torr)	5.25×10^{-48}	-	(127°C)
		-	5.3×10^{-4}	(260°C)
		-	4.9×10^{-2}	(358°C)
		1.14×10^{-14}	-	(627°C)
Heat of Formation	(kcal mol^{-1})	-141.2	-116.45	
Heat Content	(g cal)	8925	-	

* these data are shown as LiOH except molecular weight

Reference

(1) T.F. Yang, H.K. Forsen, G.A. Emmert, FDM-49 (University of Wisconsin 1975).
(2) S. Yoshikawa, N. Christofilos, Proc. of the 4th Int. Conference on Plasma Phys. and Controlled Nucl. Fusion Research, (IAEA Vienna 1971) Vol. II, p.357
(3) B.B. Kadomtsev, O.P. Pogutse, Nuclear Fusion 11, 67 (1971)
(4) S. Yoshikawa, MATT-959 (Princeton University 1973)
(5) R. Hancox, J.A. Booth, CLM-R 116 (1971)
(6) J.T.D. Mitchel, N.W. George, CLM-R 121 (1972)
(7) W.W., Jr. Engle, A Users's Manual for ANISN, Report K-1693, Union Carbide Corporation, Nuclear Division, Oak Ridge, Tennesse, March 30, (1967)
(8) H.C. Honeck, ENDF/B Specifications for an Evaluated Nuclear File for Reactor Applications, BNL-50066(T-467), ENDF-102, Brookhaven National Laboratory(May, 1966, revised July 1967) (ENDF/B corrected to July 1968)
(9) Y. Seki, T. Hiraoka, to be published
(10) G.M. McCracken, S. Blow; The Shielding of Superconducting Magnets in a Fusion Reactor, CLM-R 120, August (1972)
(11) J.T. Kriese, D. Steiner; Magnet Shield Design for Fusion Reactors, ORNL-TM-4256, June (1973)
(12) Engineering Properties of INCOLOY ALLOY 800; Technical Bulletin T-40 INCO (1965)
(13) S. Oldberg, D. Sandusey, P.E. Bohabay and F.A. Comprelli, Trans ANS 1970 Annual Meeting
(14) F.A. Comprelli et al., GEAP-13517 (1969)
(15) J.M. Beeston, C.R. Brinkman, ASTM STP 484 1970 p.419
(16) M.I. Guseva, Radio Engineering and Electronic Phys. 7 (1962) p.1563
(17) T.M. Daniel and C.R. Finfgeld, Texas Tech. Conf. (1970) ORO-1171-1
(18) O. Almen and G. Bruce, Nucl. Instr. Meth. 11 (1961) 279
(19) J.W. Mellor; A Comprehensive Treatise on Inorganic and Theoretical Chemistry, Vol.II, 451 (1952) and Vol.II, Supplement II, 146 (1961)
(20) Gmelins Handbuch der Anorganischen Chemie 20, 76 (1927) and 20, Erg. 258 (1960)
(21) G.V. Samsonova; Physico-chemical Properties of Oxide (1969)